Just a very expensive breathing training? Risk of respiratory artefacts in functional connectivity-based real-time fMRI neurofeedback

Franziska Weiss [a,*], Vera Zamoscik [a,b], Stephanie N.L. Schmidt [a,c], Patrick Halli [a], Peter Kirsch [a,d,e], Martin Fungisai Gerchen [a,d,e]

[a] Department of Clinical Psychology, Central Institute of Mental Health, University of Heidelberg/Medical Faculty Mannheim, Mannheim, Germany
[b] Department of Psychology, University of Bonn, Bonn, Germany
[c] Department of Psychology, University of Konstanz, Konstanz, Germany
[d] Department of Psychology, Heidelberg University, Heidelberg, Germany
[e] Bernstein Center for Computational Neuroscience Heidelberg/Mannheim, Mannheim, Germany

ARTICLE INFO

ABSTRACT

Real-time functional magnetic resonance imaging neurofeedback (rtfMRI NFB) is a promising method for targeted regulation of pathological brain processes in mental disorders. But most NFB approaches so far have used relatively restricted regional activation as a target, which might not address the complexity of the underlying network changes. Aiming towards advancing novel treatment tools for disorders like schizophrenia, we developed a large-scale network functional connectivity-based rtfMRI NFB approach targeting dorsolateral prefrontal cortex and anterior cingulate cortex connectivity with the striatum.

In a double-blind randomized yoke-controlled single-session feasibility study with N = 38 healthy controls, we identified strong associations between our connectivity estimates and physiological parameters reflecting the rate and regularity of breathing. These undesired artefacts are especially detrimental in rtfMRI NFB, where the same data serves as an online feedback signal and offline analysis target.

To evaluate ways to control for the identified respiratory artefacts, we compared model-based physiological nuisance regression and global signal regression (GSR) and found that GSR was the most effective method in our data.

Our results strongly emphasize the need to control for physiological artefacts in connectivity-based rtfMRI NFB approaches and suggest that GSR might be a useful method for online data correction for respiratory artefacts.

1. Introduction

In recent years the development of real-time fMRI neurofeedback (rtfMRI NFB) approaches is transforming fMRI from a knowledge-generating technology into a neurobiological intervention tool for mental disorders (Bagarinao et al., 2006; Kohl et al., 2019; Paret et al., 2019; Weiskopf et al., 2003). In rtfMRI NFB, covert brain processes are displayed in near real-time to make them accessible for targeted regulation by participants in the MRI scanner. However, the plethora of potential confounding noise sources in fMRI, like respiratory artefacts, requires special caution in the development of meaningful rtfMRI NFB approaches.

Lately, a growing number of studies could demonstrate the general ability of rtfMRI NFB to change neural activation patterns related to aberrant brain function in mental disorders (Ramot et al., 2017; Young et al., 2018; Zilverstand et al., 2017). For example, recent rtfMRI NFB studies could show that the NFB procedure induced changes in the activity of targeted brain areas (Karch et al., 2015, 2019; Kirsch et al., 2016). Several rtfMRI NFB studies have been carried out with schizophrenic (SCZ) patients as a target population. It was found that these patients were able to downregulate activity of the superior temporal gyrus (Orlov et al., 2018), upregulate the insula (Ruiz et al., 2013), or control anterior cingulate cortex (ACC) activity (Cordes et al., 2015) during rtfMRI NFB. Additionally, a recent study demonstrated a heightened pairing of default mode network (DMN) and language areas because of rtfMRI NFB (Zweerings et al., 2019).

However, most rtfMRI NFB research has hitherto mainly focused on regional BOLD activation as the target process (Caria et al., 2012; Dyck et al., 2016; Karch et al., 2015; Nicholson et al., 2017; Paret et al., 2016). Although alterations in brain connectivity has been identified as a relevant mechanism in many mental disorders (Braun et al., 2018; Fornito and Bullmore, 2015), much fewer studies have utilized functional connectivity (FC) measures (Megumi et al., 2015; Yamashita et al., 2017; Zhao et al., 2019) and even fewer studies used more complex measures like network-based approaches (Ramot et al., 2017) or effective connectivity (Koush et al., 2013, 2017). Thus, rtfMRI NFB requires further development until fully its potential of translating the results obtained with modern fMRI analysis methods like network analysis into directed interventions for regulating and normalizing distributed and complex brain processes in mental disorders is achieved.

Despite even higher risks of confounding noise effects accompanying more complex rtfMRI NFB approaches, the development of such methods might be a path worth following to address complex pathological neural phenotypes. These include changes in large scale neural networks in mental disorders such as Major Depressive Disorder (Kaiser et al., 2015), ADHD (Qian et al., 2019), or SCZ. SCZ has been characterized for a long time as a network disorder of brain dysconnectivity (Friston et al., 2016; Friston and Frith, 1995; Pettersson-Yeo et al., 2011), including reduced connectivity of frontal with subcortical regions of which frontostriatal hypoconnectivity is most prominent (Lin et al., 2018; Shukla et al., 2019; Su et al., 2013). Patients with schizophrenia are showing aberrant extra-striatal connectivity during psychosis, for example decreased FC of the putamen with right anterior insula and dorsal prefrontal cortex (Peters et al., 2017). Moreover, there is evidence of a relationship between decreased ventral striatum – ACC FC and SCZ symptoms (Lin et al., 2018). First-episode psychosis patients had lower FC between the putamen and anterior cingulate cortex, and this connectivity was predictive for the further development of negative symptoms and general functioning (Oh et al., 2019). Consequently, disease-related brain networks might be a promising target for connectivity-based rtfMRI NFB in SCZ.

As a first step towards this goal we developed a novel large-scale network connectivity-based rtfMRI NFB approach to target frontostriatal connectivity deficits of the DLPFC and ACC with the striatum in SCZ and applied the method in a preregistered double-blind randomized yoke-controlled single-session pilot study with healthy controls (N = 38) which we report here. In this manuscript we were unable to test our preregistered hypotheses, because during analysis we realized the presence of massively confounding physiological, especially respiratory, effects in the data. While we applied online motion parameter regression, spike regression of volumes affected by frame-to-frame movement, and regression of a cerebrospinal fluid (CSF) signal to clean the NFB signal from confounding factors, we did not collect prior measures to address physiological contamination of the feedback signal.

Importantly, the BOLD signal can be influenced by a variety of sources that can be labelled as noise. Examples of noise include structured noise i.e. gross subject movement and physiological sources (e.g. respiration and cardiac features) (Liu, 2016) as well as random noise (e.g. thermal noise). Unsurprisingly, it is longstanding knowledge that retrospective corrections should be applied to the data to ensure reasonable quality of the findings - a notion pointed out in 1995 (Hu et al., 1995).

Especially rtfMRI NFB methods using FC-based signals as the feedback source face a number of methodological problems which might be more pronounced than in activation-based feedback (Power et al., 2012; Power et al., 2015). In the analysis of FC-fMRI data, particularly physiological artefacts that strongly affect connectivity must be considered (Nikolaou et al., 2016). Physiological features such as heart rate and respiration mostly influence the connectivity of resting state networks (Chu et al., 2018; Nikolaou et al., 2016), underlining the need to control for these factors.

The experimental procedures we based our study on, however, are in line with general procedures in the fMRI field. While motion correction is nowadays applied by default in fMRI analyses, physiological noise correction is still conducted only in a much smaller, although growing, number of studies. This is despite physiological artefacts forming one of the largest proportions of noise in general (Kruger and Glover, 2001). Therefore, in rtfMRI NFB, it is of large interest to subtract as many of these noise sources as possible from the data as the outcome of the whole procedure strongly depends on the validity of the feedback signal. Failure to correct for any of these sources might bias the whole procedure towards training unwanted strategies that are relatively easy to apply for participants, like changing breathing patterns.

Alarmed by our findings of confounding physiological effects, we tried to identify possible ways to control the identified confounding effects in our data and present the results of analyses with two different techniques for physiology correction, namely global signal regression (GSR) (Aguirre, Zarahn, & D'Esposito, 1998; Power et al., 2015) and model-based correction for physiological noise signals with the TAPAS PhysIO Toolbox (Kasper et al., 2017).

2. Methods

2.1. Participants

Healthy participants with normal or corrected-to-normal vision, eligible for MRI scanning, and without a history of mental or neurological disorders, prior and current psychiatric diagnoses, pregnancy, or acute intake of any medication except for oral contraceptives were recruited from the student population at Mannheim and Heidelberg. Two participants of the original sample of N = 40 had to be excluded from analysis due to technical problems that occurred during scanning and N = 38 healthy participants (23 women; age: 23.39 ± 4.24 years; age range: 18–35) were analyzed. Before participation, the experimental procedures were explained and participants provided written informed consent. During the experiment, participants were automatically assigned in a double-blind procedure to one of the two experimental groups: real neurofeedback (real NFB) or yoke neurofeedback (yoke group) through a predefined randomization list. The study was approved by the Ethics Committee of the Medical Faculty Mannheim at the University of Heidelberg, Germany (2018-520N-MA) and all procedures complied with the World Medical Association's Declaration of Helsinki.

2.2. Preregistration

The study was originally planned for testing the capability of participants to modulate the target network with rtfMRI NFB and was preregistered at the Open Science Foundation (OSF NeCoSchi https://osf.io/d6fre/). The confounding physiological effects described in this paper were not expected a priori and thus not preregistered, thus the reported analyses are exploratory.

2.3. Data/code availability statement

Raw fMRI data cannot be made publicly available due to protection of sensitive personal data. The summary data the analyses were based on are available at the OSF project site. We further provide the code to estimate the summarizing respiratory parameters at the OSF project site (OSF NeCoSchi https://osf.io/d6fre/).

2.4. MRI scanning

MRI scanning was conducted at two 3T Siemens Trio TIM Scanners (Siemens Healthineers, Erlangen, Germany) at the Central Institute of Mental Health in Mannheim, Germany. MR images were obtained with a 32-channel head-coil. T1-weighted structural images were acquired with a repetition time of TR = 2.3 s, echo time of TE = 3.03 ms, flip angle = 9°, 192 slices, slice thickness = 1 mm, voxel dimensions = 1 x 1 × 1 mm³, FOV = 256 × 256 mm and a matrix size = 256 x 256. BOLD signals were measured using an echo planar imaging (EPI) sequence with TR = 1.64s,

TE $= 30$ ms, flip angle $= 73°$. The whole brain was partitioned in 30 axial slices (3 mm of thickness) with a voxel size of $3 \times 3 \times 3$ mm^3 and a field of view of 192 mm. All functional runs were acquired with the same EPI sequence.

2.5. Brain network definition

We focused the rtfMRI NFB approach and our further analyses on a bilateral network comprising the dorsolateral prefrontal cortex (DLPFC), the anterior cingulate cortex (ACC) and the striatum. The ACC was defined based on the Neuromorphometrics Atlas included in SPM12 (Wellcome Department of Cognitive Neurology, London, UK). The DLPFC was extracted from an automatical metaanalysis with Neurosynth (https ://neurosynth.org/; Yarkoni et al., 2011) on the term 'DLPFC'. In the next step we used the brain parcellations by Schaefer et al. (2018) for the cortical regions and by Choi et al. (2012) for the striatum and extracted the ROIs that fell into the defined regions, providing 22 DLPFC ROIs, 23 ACC ROIs, and 13 striatum ROIs in both hemispheres which adds up to a total of 58 regions. Both approaches that we used are based on the 7-network parcellation of the cerebral cortex by Yeo et al. (2011). While this network definition procedure is relatively complex, it was chosen because we are aiming toward developing the basis for a flexible network-based neurofeedback approach that enables the estimation of complex graph-theoretical network measures and allows identification of potential sub-networks to further refine target networks.

2.6. rtfMRI NFB training

MRI scanning was conducted in a single session. Before scanning, participants provided demographic information and answered questionnaires including the German Version of the Beck Depression Inventory-II (BDI-II) (Beck et al., 1996), the NEO Five-Factor Inventory (NEO-FFI) (Costa Jr and McCrae, 2008), Schizotypal Personality Questionnaire (SPQ) (Raine, 1991) and a sensory inventory (Zamoscik et al., 2017).

The scanning session comprised a 5:21 min T1-weighted anatomical MPRAGE scan, a resting state run, two NFB runs, and a transfer run of 9:29 min each. During the resting state measurement a fixation cross was shown at the center of the screen and participants were instructed to keep their eyes open while not thinking about specific things. A transfer run is often included in NFB experiments to test whether regulation ability transfers to situations without feedback. In our case the transfer run was exactly similar to the resting state run except that participants were instructed to use the strategies learned in the NFB runs to upregulate the target network. During NFB, a thermometer display was presented on the left and right side of a fixation cross and continuously updated every TR. This feedback signal showed averaged dynamic FC of DLPFC/ACC ROIs with striatum ROIs, and participants were instructed to upregulate the feedback signal. Participants in the yoke control group did not receive

their own feedback signal, but the saved signal of a participant from the real NFB group. Data of participants from the real group were saved in a first in first out queue, meaning that each recorded signal is used once in the yoke procedure, and a yoke participant always receives the first unused recorded signal. To ensure availability of data for the yoke procedure, the first three participants were assigned to the real feedback group. After completion of the scanning session, participants were interviewed, and group assignment was disclosed. For a graphical representation of the experimental setup and design, please see Fig. 1.

2.7. Online data analysis

All online and offline analyses were conducted in MATLAB (R2017a, MathWorks Inc., Sherborn, MA, USA). Online rtfMRI NFB processing was conducted with in-house software based on SPM12 functions.

During the resting state scan, the acquired anatomical image was segmented and normalized to the SPM 12 TPM template. The inverse projection of the normalization was then applied to map the ROI masks into individual subject space. During rtfMRI NFB scanning each newly acquired volume was directly written to the analysis laptop and realigned to the first volume of the series. Then, averaged intensity values from all ROIs in this image were extracted and added to the ROI signal time series. At each step a general linear model (GLM) was applied over the whole available data to correct for movement parameters estimated during realignment, a cerebrospinal fluid (CSF) signal, and spikes associated with head movements (framewise displacement (FD) > 0.5 mm). Fisher Z-transformed Pearson correlations were then calculated from the last 30 points (i.e. implementing a sliding window size of 30 vol) of the corrected time courses of all cortical ROIs with all striatal ROIs and averaged to determine the feedback value presented to the participant. To assure availability of sufficient data for the online correction algorithm, the first feedback value was calculated after 37 vol (60.68 s). The feedback signal was only calculated from windows that included at least 15 vol not affected by head motions (FD < 0.5 mm), otherwise the feedback value would not be estimated and the thermometer display would be kept constant until a window with sufficient data occurs.

2.8. Offline data analysis

Offline data analysis was conducted with SPM 12 (v7219). The anatomical image was segmented and normalized to SPM 12 TPM template MNI space. The first 15 vol of the functional data were discarded and the functional images were slice-time corrected, realigned, co-registered to the MPRAGE, normalized, and smoothed with an isotropic Gaussian kernel of 6 mm full width at half maximum.

A first level GLM was set up that included six movement parameters, the CSF signal, and dummy regressors for volumes affected by head motion (framewise displacement > 0.5 mm; scan-to-scan global signal
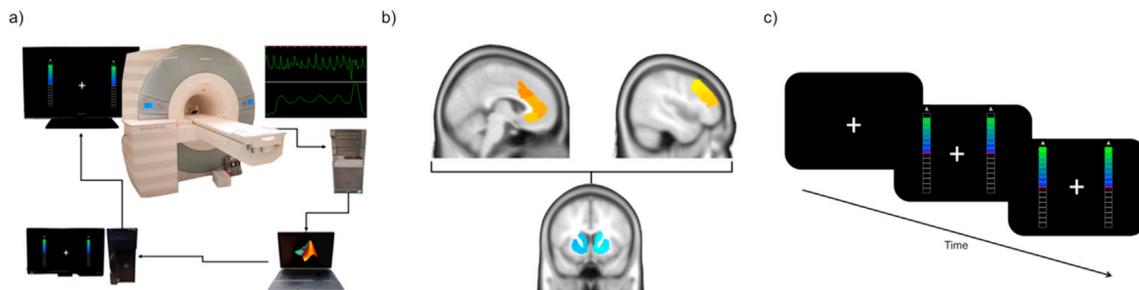

Fig. 1. Experimental setup and design. a) rtfMRI Neurofeedback Setup. Acquired images are reconstructed and sent to a laptop running in-house MATLAB scripts to preprocess the images and extract the neurofeedback signal. The feedback is sent to a computer running Presentation software and presented to the participant in the scanner as a thermometer value. During scanning physiology measures (respiration and cardiac) are recorded. b) Target Network. The feedback signal represented the averaged functional connectivity of ROIs in the ACC (upper left) and the DLPFC (upper right) with ROIs in the striatum (below). c) Experimental Design. A fixation cross is shown to the participant in the scanner. After approximately 1 min, the feedback signal is displayed as a thermometer value. This value is constantly adapted to represent the latest FC value estimated from the last 30 volumes. During resting state and transfer runs, only the fixation cross is presented.

change z > 4) and a constant. Runs which exceeded a level of 20% movement-affected volumes were excluded from further analysis (3 runs in 3 subjects). Runs with problems with physiology recording were also excluded from analysis (2 runs in 2 subjects).

To assess possible methods to correct for physiological associations, the analyses were repeated with global gray matter signal regression (GSR), model-based physiological nuisance regression (Physio), as well as both (Physio & GSR) implemented in the first level model. To be more comprehensive we also added a repetition with white matter signal regression (WMR). Then, the time courses from the ROIs used in the online NFB procedure were extracted from the residual images of the first level analyses and large-scale network connectivity was estimated from averaged Fisher Z-transformed Pearson correlations between the DLPFC/ACC ROIs and the striatal ROIs.

Second level analyses were conducted based on these DLPFC/ACC-striatum large-scale network connectivity values. In all second level analyses, age, gender and scanner were included as covariates. For group comparisons, we used two-sample t-tests implemented in a GLM model, which allowed for the addition of covariates. Associations of connectivity values with physiological parameters were assessed with partial correlations. As our main analyses are aiming at demonstrating confounding physiological effects, we did not correct the reported p-values for multiple comparisons, because multiple comparison correction might potentially hide nuisance effects in this case.

2.9. Physiological noise correction

Respiration and heart rate were recorded with a pulse finger clip and a respiration belt during MRI at a sampling rate of 50 Hz using built-in equipment (PMU Wireless Physio Control, Siemens Healthineers, Erlangen, Germany). Before estimating physiological parameters, we cut the physiological recordings based on recorded volume triggers so that they were exactly aligned with the analyzed fMRI data. Then we used the TAPAS PhysIO Toolbox (Kasper et al., 2017; https://doi.org/10.1016/j.jneumeth.2016.10.019) to estimate 20 physiological nuisance regressors, including cardiac, respiratory, cardiac × respiratory interaction (RETROICOR order 1), heart rate variability (HRV; RETROICOR order 3), and respiratory volume per time (RVT; RETROICOR order 4) terms. The derived physiology nuisance regressors were included in the first level GLM of the respective analyses (see above), and an F contrast over all physiology regressors was estimated to test whether physiology correction worked (see Supplementary Fig. 1 for six examples.). We also repeated the analyses with a more complex model with 39 regressors that included temporally shifted versions of the respiratory response function before convolution with RVT (shifts from -24 s to 18 s in 6 s steps and additional shifts of -3 s, -1 s, 1 s and 3 s) and HRV as described by Biancardi et al. (2009).

2.10. Physiological parameters

While the PhysIO toolbox provides physiology time courses, we also calculated additional summarizing respiratory and cardiac parameters from the time courses that are potentially associated with the BOLD signal (Zamoscik et al., 2018) to test for confounding associations over subjects.

We created a set of respiration parameters: Breath Rate (peaks/breaths per minute), expiratory pause duration, its variance, and expiration-to-inspiration time ratio. For these parameters, expiration was defined as starting at each maximum peak and ending at the lowest local minimum before the next maximum peak, and correspondingly, inspiration was defined as the opposite. With these data we calculated the expiration-to-inspiration time ratio. For detecting expiratory pauses, we calculated the slope of the respiration curve with a sliding window approach (window size of 5 samples) to find clusters of minimum peaks which were then used to determine rough temporal markers for a provisional pause onset. This was recursively extended into both directions

based on the slope parameters to determine pause onset and offset. In addition to the expiratory pause duration, we calculated the coefficient of variance (standard deviation divided by the mean) of pause duration (Pause CV; see Supplementary Fig. 5). For a more detailed description of the respiratory parameters please see also (Zamoscik et al., 2018). Additionally, we estimated heart rate (beats per minute) and two heart rate variability parameters, namely the standard deviation of the length of all beat intervals (SDNN [ms]) and the root mean square of successive differences of intervals (RMSSD [ms]).

3. Results

3.1. Functional connectivity group comparison

Connectivity estimates of the NFB runs were compared between the experimental groups with a one-sided independent samples t-test in accordance with the preregistered hypotheses. Higher large-scale network connectivity between DLPFC/ACC and striatum was found in the real NFB group in comparison to the yoke group during the first NFB run (NFB1: t (31) = 1.81, p = .040). Comparisons of connectivity estimates of the second NFB and the transfer run did not yield significant effects (NFB2: t (32) = 0.66, p = .258; transfer: t (30) = 0.615, p = .277). After including physiological nuisance regressors estimated with the PhysIO toolbox in the first level model, the group comparison of NFB1 remained significant (t (31) = 1.70, p = .049). However, when GSR or GSR and physiology correction combined were applied to the data, the effect in the first NFB run was no longer significant (GSR: t (31) = 1.09, p = .142; GSR and physiology correction: t (31) = 0.84, p = .205) (see Fig. 2 and Supplementary Fig. 12).

3.2. Physiological associations

3.2.1. Correlations between physiology measures and functional connectivity
We then investigated the correlations of physiological measures with the target FC of the respective runs. These analyses were conducted separately for each correction method. Here we report the associations with Breath Rate, Pause CV and RMSSD in the first NFB run. The results for the other parameters and the other runs are similar and are presented in detail in the supplement.

3.2.2. Data not corrected for physiology
The analyses consistently showed strong significant correlations of respiratory physiological parameters with the target FC during NFB1 (see Fig. 3, a and e and Supplementary Figs. 4–7 for all runs). Cardiac parameters showed no correlation with our FC estimate in NFB1 (RMSSD: rho = −0.026, p = .888) (see Fig. 4, a), but a relatively weak association in the resting state data (Supplementary Figs. 8–10).

3.2.3. Physio correction
When physiology correction with nuisance regressors estimated with the PhysIO toolbox was used, only minor changes in the association of physiology and target FC were seen. As shown in Fig. 3 (b,f), Breath Rate and Pause CV both exhibited highly significant correlations with the target FC during NFB1 (Breath Rate: rho = −0.448, p = .009; Pause CV: rho = 0.606, p = 1.8659e-04). For further details, see Supplementary Figs. 4–7. In line with the uncorrected analyses, the cardiac parameter RMSSD showed almost no association with the respective BOLD signal (rho = −0.027, p = .883) as can be seen in Fig. 4 (Supplementary Figs. 8–10). Using a more complex model with shifted respiratory response functions did only slightly diminish these associations during NFB1 (Breath Rate: rho = -0.400, p = .023; Pause CV: rho = .477, p = .006; see Supplementary Fig. 14).

3.2.4. Global signal correction
In comparison to the previous approach, applying GSR in the first level analyses yielded non-significant correlations between target FC and
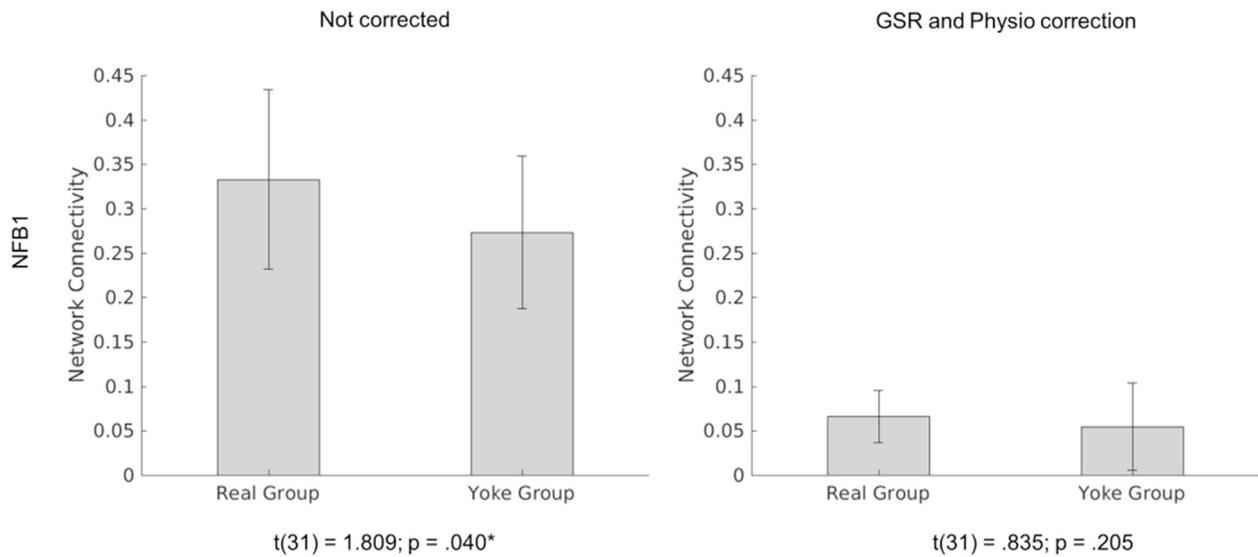
Fig. 2. Group effect in the first neurofeedback run (NFB1). a) Group comparison of network connectivity between the real NFB and yoke NFB group uncorrected for physiology. b) Group comparison of network connectivity between the real NFB and yoke NFB group in data with global signal (GSR) and model-based physiology (Physio) correction.

all parameters for respiration (Breath Rate: rho = −0.079, p = .662; Pause CV: rho = −0.060, p = .74; Fig. 3 (c, g)) and HRV (RMSSD: rho = 0.047, p = .797; Fig. 4 (c)) during NFB1 (Supplementary Figs. 4–10). In an exemplary subject we show a strong association of the global signal with the data (Supplementary Fig. 2a). In contrast to GSR, white matter regression (WMR) did not eliminate the associations during NFB1

(Breath Rate: rho = −0.27, p = .129; Pause CV: rho = 0.558, p = 7.4163e-04; see Supplementary Fig. 14).

3.2.5. Global signal and physio correction
    The combination of GSR and model-based physiology nuisance regressors likewise resulted in non-significant correlations across all
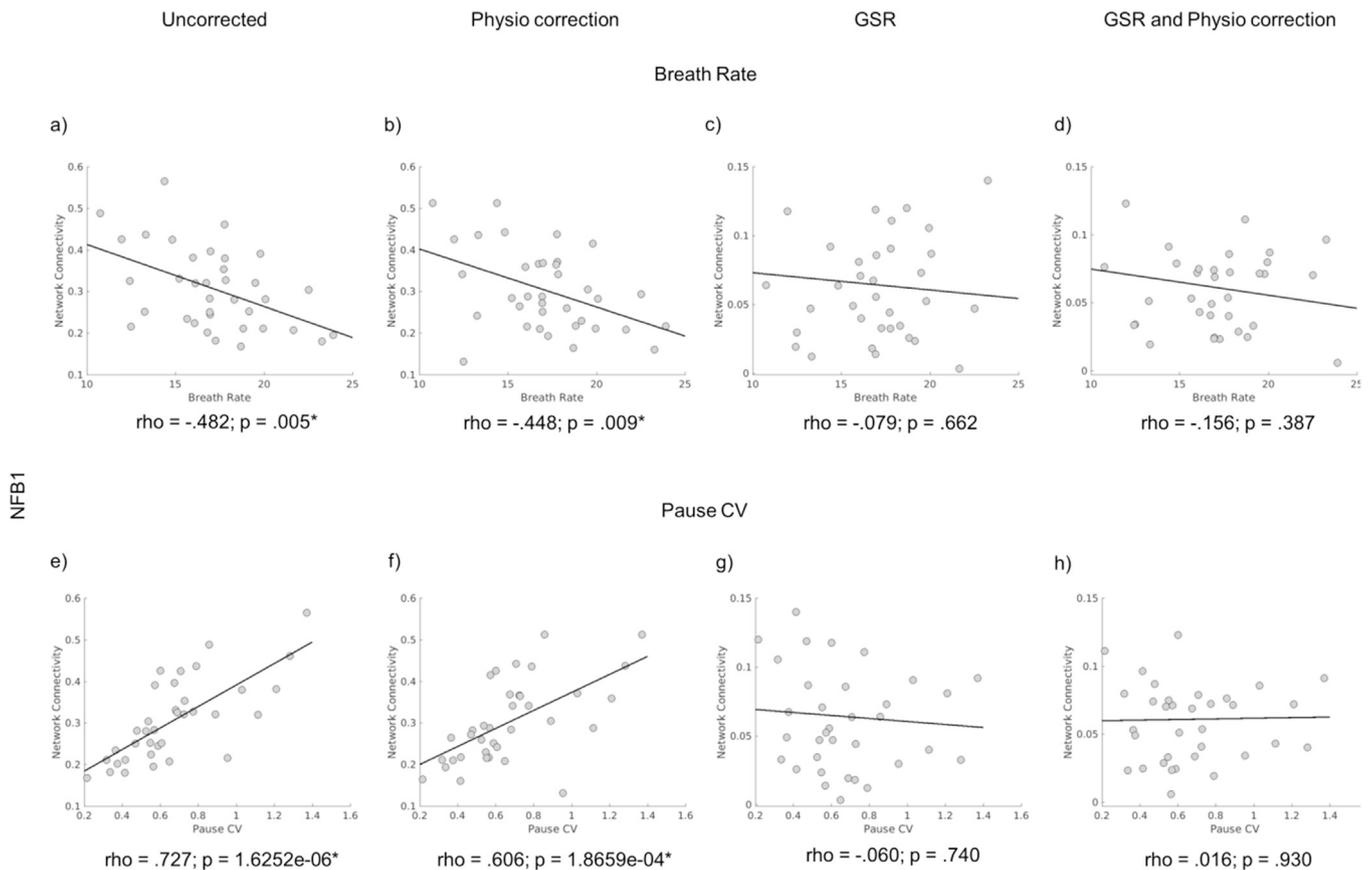

Fig. 3. Association of respiratory parameters with network connectivity in the first neurofeedback run (NFB1). Correlations of the respiratory parameters Breath Rate and Pause CV (standard deviation of respiration pause duration divided by its mean), a measure for regularity of breathing, with target network connectivity for the different physiology corrections. Physio: model-based physiology correction; GSR: global signal regression. Please note that, as expected, GSR overall shifted connectivity estimates towards 0.

Fig. 4. Association of cardiac parameters with network connectivity in NFB1. Correlations of the cardiac parameter RMSSD (root mean square of the successive differences [ms]) with target network connectivity for the different physiology corrections. Physio: model-based physiology correction; GSR: global signal regression. Please note that, as expected, GSR overall shifted connectivity estimates towards 0.
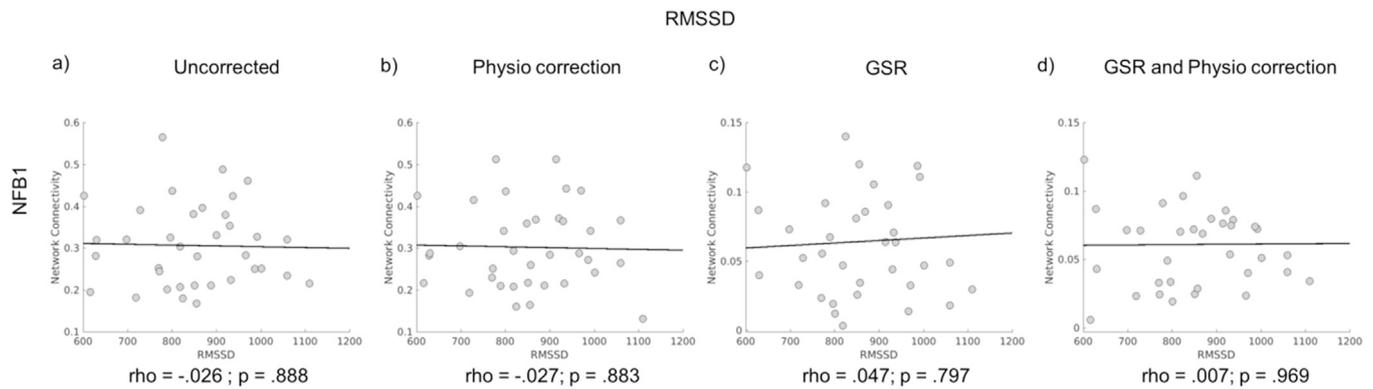
parameters (Breath Rate: rho = −0.156, p = .387; Pause CV: rho = 0.016; p = .93; RMSSD: rho = 0.007, p = .969), see Fig. 3 (d, h) and 4 (d) and Supplementary Figs. 4–10. The association of the global signal with the data is much larger than the association of model-based nuisance regressors (Supplementary Fig. 2b).

3.2.6. Change in physiological parameters between runs in the experiment

Because of the associations between respiratory parameters and connectivity estimates we explored whether respiration changed between runs differently in the groups (Supplementary Fig. 11). to identify training effects on respiratory parameters. We first tested whether the parameters changed between the resting state run and the first NFB run. On a descriptive level, Breath Rate was slightly increased in the real feedback group (mean change: .245) and even more in the yoke feedback group (mean change: 1.22), but the groups did not show significant differences in Breath Rate between rest and NFB1 (t(31) = -1.007, p = .322). However, the change in Breath Rate was negatively associated with the change in connectivity (rho = -.533, p = .001). For Pause CV, the change was significantly different between the groups (t(31) = 2.085, p = .045) with a mean change of .258 in the real group and a mean change of .017 in the yoke group. Furthermore, we found a strong relationship between Pause CV change and change in connectivity (rho = .757, p = 3.3812e-07).

Between the first NFB run and the second, we did not find significant group differences in the change of these respiratory parameters. On a descriptive level, Breath Rate was reduced in the real feedback group (mean change: 0.742) and not in the yoke group (mean change: 0.007), but the groups did not significantly differ in Breath Rate change between NFB1 and NFB2 (t (31) = −1.257, p = .218). However, the change in Breath Rate was negatively associated with the change in connectivity (rho = −0.515, p = .003). For Pause CV, the real group had a mean change of −0.064 and the yoke group of .037, and the change was also not significantly different between the groups (t (31) = −1.092, p = .283). For Pause CV there was no association between parameter change and change in connectivity (rho = 0.232, p = .201).

4. Discussion

We conducted a double-blind randomized yoke-controlled single-session pilot trial originally designed and preregistered to test the feasibility of a newly developed large-scale FC rtfMRI NFB approach targeting DLPFC/ACC-striatum FC. When testing the preregistered hypotheses we found only a weak effect in the first NFB run (NFB1). After applying corrections for physiological artefacts, this effect could not be detected any longer. This allowed us to assess the influence of physiological parameters on our FC estimates in exploratory analyses. In our data we identified worryingly strong relationships between parameters reflecting the rate and regularity of breathing and our target large-scale network FC

signature during all runs of the experiment, as well as a putative training effect on the regularity of respiration (Pause CV) from the resting state to the first NFB run.

Of note, our results are based on second-level analyses, where inter-individual differences in respiration between participants were strongly associated with differences in large-scale network connectivity. This is relevant in rtfMRI NFB because the comparison of different subjects in different groups is often used as the level of analysis, and differences in respiration or changes in respiration during NFB training might lead to false positive results. We are aware that a single NFB training session may not provide enough data to assess whether our large-scale rtfMRI NFB approach worked, or whether a training effect of physiological parameters occurred. However, we collected a sufficient amount of data to clearly identify the associations of our large-scale network FC measure with respiratory parameters.

With hindsight, these relationships should have been expected. In general, the existence of respiratory artefacts has been well described for fMRI (Caballero-Gaudes and Reynolds, 2017; Chu et al., 2018; Nikolaou et al., 2016; Power et al., 2018; Power et al., 2017). These low-frequency confounds reduce the sensitivity of the signal (Murphy et al., 2013) and are not extracted by standard physiology corrections (Birn et al., 2006) and low pass filtering (Liu et al., 2017).

Physiological artefacts have an especially heavy influence on FC estimates (Nikolaou et al., 2016). Particularly respiration effects are difficult to distinguish from FC due to identical spatial locations and temporal characteristics (Birn et al., 2006). Our target network was more strongly affected by respiration than by cardiac features, suggesting that in frontostriatal networks cardiac features have little effect on the BOLD response. Here, our results are in line with the finding that cardiac properties generally influence the global BOLD signal only to a small degree (Power et al., 2018). Whereas CSF regions and regions near greater arteries and draining veins are especially vulnerable for noise of cardiac nature (Bhattacharyya and Lowe, 2004; Birn et al., 2006; Caballero-Gaudes and Reynolds, 2017).

Thus, the consequences of respiratory artefacts are concerning and it is important to control for them. This is of even higher importance in the case of rtfMRI NFB, where the fMRI signal or a derived measure is the fed back to be modulated by the participants in addition to being the main analyzed data. If confounding effects in the feedback signal are not corrected, it might be much easier for the participants to manipulate the target signal by changing physiological parameters like breathing patterns instead of regulating brain processes. For example, Ramot et al. (2017) reported that subjects stated that they have changed their breathing patterns as a behavioral strategy to regulate the neurofeedback signal. Indeed, a common objection against rtfMRI NFB is the danger of confounding noise that might contaminate the feedback signal. Our empirical results suggest that there is indeed a real danger for respiratory artefacts, at least in connectivity-based rtfMRI NFB, which may simply

lead to a costly form of breathing training, rather than an effective NFB treatment. To identify ways to control for the unintended associations, we assessed two possible approaches to correct for the identified artefacts in our data, the inclusion of model-based physiological nuisance regressors estimated with the TAPAS PhysIO toolbox, and the simpler but also disputed inclusion of the global gray matter signal in the first level model. While we tested these approaches offline with already acquired data, we chose them because both could be implemented relatively easily in the online rtfMRI NFB procedures.

In general, the PhysIO toolbox and the regression of physiological nuisance parameters seemed to work at least satisfactorily. F-contrasts over all physiological regressors included in the respective first level analyses showed strong relationships with the data, with only very few runs showing weak relationships (see Supplementary Fig. 1). However, the model-based physiology corrections resulted in virtually no change of the second level association of connectivity estimates with physiological parameters. This was surprising, as the model-based approach represents the current state-of-the-art for physiology correction. It nonetheless seems relatively unlikely that this was due to failures in the application of the toolbox or in the toolbox itself. We have carefully double-checked our analyses, and even if physiology correction did not work as perfectly as possible, the large amount of variance removed together with its very small influence on the second level associations makes it unlikely that this would be substantially changed if the removed variance would not be increased much further. Nonetheless, we cannot exclude the possibility that the used physiological recordings are not of optimal quality as the built-in recording devices probably provide suboptimal measurements which could influence the quality of the model-based physiological correction. However, our data quality should be at a comparative standard level and reflect the level available at other sites with similar standard equipment.

In comparison to model-based physiology correction, model-free GSR was capable of attenuating the associations between the same physiology parameters and target measure sufficiently, resulting in non-significant correlations. The association was even further attenuated when a combination of GSR and Physio correction was used. GSR seemed to reduce variance in both groups, as well as the mean difference between groups. After GSR the residual variance in the first NFB run seems to be relatively larger in the yoke group than in the real group (Fig. 2), which might be expected. Participants in the yoke group have no control about the brain process they try to regulate. Therefore, they should apply diverse strategies that randomly influence the target process and increase variance.

Several issues might be related to the difference between the model-based and model-free GSR approaches. An apparent difference between GSR and Physio correction is the strength of association with the data, and thus the amount of variance removed by the approaches, which is much larger for GSR (Supplementary Fig. 2). This might reflect the ability of the global signal to capture more noise in the data than the model-based physiology nuisance regressors. Another possibility might be that the intraindividual physiology nuisance regressors do not eliminate interindividual differences in the baseline of physiological parameters, which are then taken up by the second level analyses at the group level. Furthermore it was recently shown that the used measure of respiratory volume over time (RVT) can have inferior correction performance for respiratory artefacts in comparison to alternative approaches like RVT envelope of the waveform or windowed variance in the waveform (Power et al., 2020)**, which might provide an explanation for the failure of the physiological model to capture much variance in this study**There is also the option that a real relationship between respiration and the target brain process exists, and that the frontostriatal network is in fact controllable by changing respiration, or that another brain region controls both, the network and respiration.

It should be noted that our results are not in line with the report of Hellrung (2018) who conclude that in activation-based rtfMRI NFB of the amygdala training effects are not mainly driven by physiological artefacts. It might be the case that our large-scale network NFB approach is specifically sensitive for the artefacts.

Taken together, in our analyses GSR was the single most effective method to correct for the undesired physiological associations that we detected in the group data. This fits to prior research emphasizing the ability of GSR to capture not only the activity of voxels located in the major clusters of the brain (Chen et al., 2012), but also reflects noise of different origins i.e. scanner driven-noise, motion, respiratory and heart-rate (Murphy and Fox, 2017).

According to Zarahn et al. (1997) inclusion of the global signal as a covariate decreases the effects of spatially related noise, which again allows for a better detection of effects in fMRI studies (Aguirre et al., 1997). Interestingly, after correlating the global signal with fMRI data, Birn et al. (2006) found that these maps were identical to maps of regions with signs of respiration. These correlations were particularly strong in gray matter regions elucidating the need to take this knowledge into account for fMRI analyses. GSR has also been suggested recently as a method to correct for noise of respiratory nature in modern multi-echo fMRI sequences (Power et al., 2018), although this has been debated (Power et al., 2019; Spreng et al., 2019).

Despite the ability of GSR for noise correction, it remains a controversial technique because it is unclear what the global signal in fact measures. As it is a hard problem to delineate low-frequency artefacts from neural effects, real signal could potentially be removed by the method (Hahamy et al., 2014). Another common remark about GSR is that it might induce spurious negative correlations (Saad et al., 2012), e.g. of task-negative and task-positive networks (Fox et al., 2009). However, similar negative correlations might also appear when only physiological noise correction is applied (Chang and Glover, 2009) and some negative correlations might reflect real neural signal instead of artefacts (Chai et al., 2012).

However, it has to be noted that GSR may skew results in clinical populations. It was shown that the global signal is changed in SCZ, although it is unclear in which direction the changes occur, since opposing results were reported (Hahamy et al., 2014; Yang et al., 2014). While Caballero-Gaudes and Reynolds (2017) emphasize caution in the application of GSR to task-based activity or FC, it currently seems to be the most effective approach for eliminating global artefacts (Power et al., 2017) and shows superior output than different state-of-the-art correction methods, like e.g. ICA in terms of eliminating motion artefacts (Burgess et al., 2016; Liu et al., 2017).

So far it remains unclear how well GSR would work in rtfMRI NFB, and which correction method is providing the best online signal for learning to modulate brain networks. Thus, further research is needed to replicate the results and better understand the reported effects.

It is also crucial to mention that respiration is indeed truly associated with neural activity (Heck et al., 2016; Herrero et al., 2018; Ito et al., 2014) and the removal of the respiratory signal might thus also result in the loss of actual neural information. The reasons why we consider all physiological associations as artefacts here are that it is not clear how nuisance and real effects could be separated, and that rtfMRI is probably too costly to be the method of choice to measure and feedback signals that are strongly coupled to respiration, which could be assessed in a more direct and cheaper way.

Importantly, it was only possible to identify and examine the relationships between FC and physiology in this study because we recorded physiological parameters during fMRI scanning, otherwise the detected associations might have gone unnoticed. It thus follows as a clear recommendation for fMRI NFB research that physiological signals are recorded during scanning, and that the contamination of the target signal by physiological parameters is assessed and reported. To foster replication and further research on this topic we provide the scripts that we used to estimate physiological parameters as an open source script.

5. Conclusion

Our results suggest that it might be necessary to account for

physiological artefacts in connectivity-based rtfMRI NFB, for example by applying online GSR. Failures in correction of physiological artefacts from online signals might lead to a confounded feedback which undermines the methodology of a study and challenges the validity of the conclusions. Given the massive impact physiological artefacts have on the BOLD signal, caution seems to be needed when interpreting the results of studies that do not use working physiology correction.

Funding

Declaration of competing interest

The authors declare that they have no known competing financial interests or personal relationships that could have appeared to influence the work reported in this paper.

CRediT authorship contribution statement

Franziska Weiss: Conceptualization, Formal analysis, Investigation, Methodology, Validation, Visualization, Writing - original draft, Writing - review & editing. **Vera Zamoscik:** Writing - original draft, Methodology, Software. **Stephanie N.L. Schmidt:** Software. **Patrick Halli:** Visualization. **Peter Kirsch:** Conceptualization, Investigation, Writing - original draft, Project administration, Funding acquisition, Supervision. **Martin Fungisai Gerchen:** Conceptualization, Formal analysis, Investigation, Methodology, Software, Supervision, Visualization, Writing - original draft, Writing - review & editing.

Acknowledgements

Appendix A. Supplementary data

Supplementary data to this article can be found online at https://doi.org/10.1016/j.neuroimage.2020.116580.

References

Aguirre, G.K., Zarahn, E., D'Esposito, M., 1997. Empirical analyses of BOLD fMRI statistics. II. Spatially smoothed data collected under null-hypothesis and experimental conditions. Neuroimage 5 (3), 199–212.

Aguirre, G.K., Zarahn, E., D'Esposito, M., 1998. The inferential impact of global signal covariates in functional neuroimaging analyses. Neuroimage 8 (3), 302–306. https://doi.org/10.1006/nimg.1998.0367.

Bagarinao, E., Nakai, T., Tanaka, Y., 2006. Real-time functional MRI: development and emerging applications. Magn. Reson. Med. Sci. 5 (3), 157–165. https://doi.org/10.2463/mrms.5.157.

Beck, A.T., Steer, R.A., Brown, G.K., 1996. BDI-II, Beck Depression Inventory : Manual.

Bhattacharyya, P.K., Lowe, M.J., 2004. Cardiac-induced physiologic noise in tissue is a direct observation of cardiac-induced fluctuations. Magn. Reson. Imaging 22 (1), 9–13. https://doi.org/10.1016/j.mri.2003.08.003.

Bianciardi, M., Fukunaga, M., van Gelderen, P., Horovitz, S.G., de Zwart, J.A., Shmueli, K., Duyn, J.H., 2009. Sources of functional magnetic resonance imaging signal fluctuations in the human brain at rest: a 7 T study. Magn. Reson. Imaging 27 (8), 1019–1029. https://doi.org/10.1016/j.mri.2009.02.004.

Birn, R.M., Diamond, J.B., Smith, M.A., Bandettini, P.A., 2006. Separating respiratory-variation-related fluctuations from neuronal-activity-related fluctuations in fMRI. Neuroimage 31 (4), 1536–1548. https://doi.org/10.1016/j.neuroimage.2006.02.048.

Braun, U., Schaefer, A., Betzel, R.F., Tost, H., Meyer-Lindenberg, A., Bassett, D.S., 2018. From maps to multi-dimensional network mechanisms of mental disorders. Neuron 97 (1), 14–31. https://doi.org/10.1016/j.neuron.2017.11.007.

Burgess, G.C., Kandala, S., Nolan, D., Laumann, T.O., Power, J.D., Adeyemo, B., Barch, D.M., 2016. Evaluation of denoising strategies to address motion-correlated artifacts in resting-state functional magnetic resonance imaging data from the human connectome project. Brain Connect. 6 (9), 669–680. https://doi.org/10.1089/brain.2016.0435.

Caballero-Gaudes, C., Reynolds, R.C., 2017. Methods for cleaning the BOLD fMRI signal. Neuroimage 154, 128–149. https://doi.org/10.1016/j.neuroimage.2016.12.018.

Caria, A., Sitaram, R., Birbaumer, N., 2012. Real-time fMRI: a tool for local brain regulation. Neuroscientist 18 (5), 487–501. https://doi.org/10.1177/1073858411407205.

Chai, X.J., Castanon, A.N., Ongur, D., Whitfield-Gabrieli, S., 2012. Anticorrelations in resting state networks without global signal regression. Neuroimage 59 (2), 1420–1428. https://doi.org/10.1016/j.neuroimage.2011.08.048.

Chang, C., Glover, G.H., 2009. Effects of model-based physiological noise correction on default mode network anti-correlations and correlations. Neuroimage 47 (4), 1448–1459. https://doi.org/10.1016/j.neuroimage.2009.05.012.

Chen, G., Chen, G., Xie, C., Ward, B.D., Li, W., Antuono, P., Li, S.J., 2012. A method to determine the necessity for global signal regression in resting-state fMRI studies. Magn. Reson. Med. 68 (6), 1828–1835. https://doi.org/10.1002/mrm.24201.

Choi, E.Y., Yeo, B.T., Buckner, R.L., 2012. The organization of the human striatum estimated by intrinsic functional connectivity. J. Neurophysiol. 108 (8), 2242–2263. https://doi.org/10.1152/jn.00270.2012.

Chu, P.P.W., Golestani, A.M., Kwinta, J.B., Khatamian, Y.B., Chen, J.J., 2018. Characterizing the modulation of resting-state fMRI metrics by baseline physiology. Neuroimage 173, 72–87. https://doi.org/10.1016/j.neuroimage.2018.02.004.

Cordes, J.S., Mathiak, K.A., Dyck, M., Alawi, E.M., Gaber, T.J., Zepf, F.D., Mathiak, K., 2015. Cognitive and neural strategies during control of the anterior cingulate cortex by fMRI neurofeedback in patients with schizophrenia. Front. Behav. Neurosci. 9, 169. https://doi.org/10.3389/fnbeh.2015.00169.

Costa Jr., P.T., McCrae, R.R., 2008. The NEO inventories. In: Personality Assessment. Routledge/Taylor & Francis Group, New York, NY, US, pp. 213–245.

Dyck, M.S., Mathiak, K.A., Bergert, S., Sarkheil, P., Koush, Y., Alawi, E.M., Mathiak, K., 2016. Targeting treatment-resistant auditory verbal hallucinations in schizophrenia with fMRI-based neurofeedback - exploring different cases of schizophrenia. Front. Psychiatr. 7, 37. https://doi.org/10.3389/fpsyt.2016.00037.

Fornito, A., Bullmore, E.T., 2015. Reconciling abnormalities of brain network structure and function in schizophrenia. Curr. Opin. Neurobiol. 30, 44–50. https://doi.org/10.1016/j.conb.2014.08.006.

Fox, M.D., Zhang, D., Snyder, A.Z., Raichle, M.E., 2009. The global signal and observed anticorrelated resting state brain networks. J. Neurophysiol. 101 (6), 3270–3283. https://doi.org/10.1152/jn.90777.2008.

Friston, K., Brown, H.R., Siemerkus, J., Stephan, K.E., 2016. The dysconnection hypothesis (2016). Schizophr. Res. 176 (2–3), 83–94. https://doi.org/10.1016/j.schres.2016.07.014.

Friston, K.J., Frith, C.D., 1995. Schizophrenia: a disconnection syndrome? Clin. Neurosci. 3 (2), 89–97.

Hahamy, A., Calhoun, V., Pearlson, G., Harel, M., Stern, N., Attar, F., Salomon, R., 2014. Save the global: global signal connectivity as a tool for studying clinical populations with functional magnetic resonance imaging. Brain Connect. 4 (6), 395–403. https://doi.org/10.1089/brain.2014.0244.

Heck, D.H., McAfee, S.S., Liu, Y., Babajani-Feremi, A., Rezaie, R., Freeman, W.J., Kozma, R., 2016. Breathing as a fundamental rhythm of brain function. Front. Neural Circ. 10, 115. https://doi.org/10.3389/fncir.2016.00115.

Hellrung, L., Borchardt, V., Götting, F.N., Stadler, J., Tempelmann, C., Tobler, P.N., Walter, M., van der Meer, J.N., 2018. Motion and physiological noise effects on amygdala real-time fMRI neurofeedback learning. BioRxiv 366138 [Preprint]. July 13, 2018. Available from: https://doi.org/10.1101/366138.

Herrero, J.L., Khuvis, S., Yeagle, E., Cerf, M., Mehta, A.D., 2018. Breathing above the brain stem: volitional control and attentional modulation in humans. J. Neurophysiol. 119 (1), 145–159. https://doi.org/10.1152/jn.00551.2017.

Hu, X., Le, T.H., Parrish, T., Erhard, P., 1995. Retrospective estimation and correction of physiological fluctuation in functional MRI. Magn. Reson. Med. 34 (2), 201–212.

Ito, J., Roy, S., Liu, Y., Cao, Y., Fletcher, M., Lu, L., Heck, D.H., 2014. Whisker barrel cortex delta oscillations and gamma power in the awake mouse are linked to respiration. Nat. Commun. 5, 3572. https://doi.org/10.1038/ncomms4572.

Kaiser, R.H., Andrews-Hanna, J.R., Wager, T.D., Pizzagalli, D.A., 2015. Large-scale network dysfunction in major depressive disorder: a meta-analysis of resting-state functional connectivity. JAMA Psychiatry 72 (6), 603–611. https://doi.org/10.1001/jamapsychiatry.2015.0071.

Karch, S., Keeser, D., Hummer, S., Paolini, M., Kirsch, V., Karali, T., Pogarell, O., 2015. Modulation of craving related brain responses using real-time fMRI in patients with alcohol use disorder. PloS One 10 (7), e0133034. https://doi.org/10.1371/journal.pone.0133034.

Karch, S., Paolini, M., Gschwendtner, S., Jeanty, H., Reckenfelderbaumer, A., Yaseen, O., Ruther, T., 2019. Real-time fMRI neurofeedback in patients with tobacco use disorder during smoking cessation: functional differences and implications of the first training session in regard to future abstinence or relapse. Front. Hum. Neurosci. 13, 65. https://doi.org/10.3389/fnhum.2019.00065.

Kasper, L., Bollmann, S., Diaconescu, A.O., Hutton, C., Heinzle, J., Iglesias, S., Stephan, K.E., 2017. The PhysIO toolbox for modeling physiological noise in fMRI data. J. Neurosci. Methods 276, 56–72. https://doi.org/10.1016/j.jneumeth.2016.10.019.

Kirsch, M., Gruber, I., Ruf, M., Kiefer, F., Kirsch, P., 2016. Real-time functional magnetic resonance imaging neurofeedback can reduce striatal cue-reactivity to alcohol stimuli. Addiction Biol. 21 (4), 982–992. https://doi.org/10.1111/adb.12278.

Kohl, S.H., Veit, R., Spetter, M.S., Gunther, A., Rina, A., Luhrs, M., Hallschmid, M., 2019. Real-time fMRI neurofeedback training to improve eating behavior by self-regulation of the dorsolateral prefrontal cortex: a randomized controlled trial in overweight and obese subjects. Neuroimage 191, 596–609. https://doi.org/10.1016/j.neuroimage.2019.02.033.

Koush, Y., Meskaldji, D.E., Pichon, S., Rey, G., Rieger, S.W., Linden, D.E., Scharnowski, F., 2017. Learning control over emotion networks through connectivity-based neurofeedback. Cerebr. Cortex 27 (2), 1193–1202. https://doi.org/10.1093/cercor/bhv311.

Koush, Y., Rosa, M.J., Robineau, F., Heinen, K., S, W.R., Weiskopf, N., Scharnowski, F., 2013. Connectivity-based neurofeedback: dynamic causal modeling for real-time fMRI. Neuroimage 81, 422–430. https://doi.org/10.1016/j.neuroimage.2013.05.010.

Kruger, G., Glover, G.H., 2001. Physiological noise in oxygenation-sensitive magnetic resonance imaging. Magn. Reson. Med. 46 (4), 631–637.

Lin, P., Wang, X., Zhang, B., Kirkpatrick, B., Ongur, D., Levitt, J.J., Wang, X., 2018. Functional dysconnectivity of the limbic loop of frontostriatal circuits in first-episode, treatment-naive schizophrenia. Hum. Brain Mapp. 39 (2), 747–757. https://doi.org/10.1002/hbm.23879.

Liu, T.T., 2016. Noise contributions to the fMRI signal: an overview. Neuroimage 143, 141–151. https://doi.org/10.1016/j.neuroimage.2016.09.008.

Liu, T.T., Nalci, A., Falahpour, M., 2017. The global signal in fMRI: nuisance or Information? Neuroimage 150, 213–229. https://doi.org/10.1016/j.neuroimage.2017.02.036.

Megumi, F., Yamashita, A., Kawato, M., Imamizu, H., 2015. Functional MRI neurofeedback training on connectivity between two regions induces long-lasting changes in intrinsic functional network. Front. Hum. Neurosci. 9, 160. https://doi.org/10.3389/fnhum.2015.00160.

Murphy, K., Birn, R.M., Bandettini, P.A., 2013. Resting-state fMRI confounds and cleanup. Neuroimage 80, 349–359. https://doi.org/10.1016/j.neuroimage.2013.04.001.

Murphy, K., Fox, M.D., 2017. Towards a consensus regarding global signal regression for resting state functional connectivity MRI. Neuroimage 154, 169–173. https://doi.org/10.1016/j.neuroimage.2016.11.052.

Nicholson, A.A., Rabellino, D., Densmore, M., Frewen, P.A., Paret, C., Kluetsch, R., Lanius, R.A., 2017. The neurobiology of emotion regulation in posttraumatic stress disorder: amygdala downregulation via real-time fMRI neurofeedback. Hum. Brain Mapp. 38 (1), 541–560. https://doi.org/10.1002/hbm.23402.

Nikolaou, F., Orphanidou, C., Papakyriakou, P., Murphy, K., Wise, R.G., Mitsis, G.D., 2016. Spontaneous physiological variability modulates dynamic functional connectivity in resting-state functional magnetic resonance imaging. Philos Trans A Math Phys Eng Sci 374 (2067). https://doi.org/10.1098/rsta.2015.0183.

Oh, S., Kim, M., Kim, T., Lee, T.Y., Kwon, J.S., 2019. Resting-state functional connectivity of the striatum predicts improvement in negative symptoms and general functioning in patients with first-episode psychosis: a 1-year naturalistic follow-up study. Aust. N. Z. J. Psychiatr. https://doi.org/10.1177/0004867419885452, 4867419885452.

Orlov, N.D., Giampietro, V., O'Daly, O., Lam, S.L., Barker, G.J., Rubia, K., Allen, P., 2018. Real-time fMRI neurofeedback to down-regulate superior temporal gyrus activity in patients with schizophrenia and auditory hallucinations: a proof-of-concept study. Transl. Psychiatry 8 (1), 46. https://doi.org/10.1038/s41398-017-0067-5.

Paret, C., Goldway, N., Zich, C., Keynan, J.N., Hendler, T., Linden, D., Kadosh, K.C., 2019. Current progress in real-time functional magnetic resonance-based neurofeedback: methodological challenges and achievements. Neuroimage, 116107. https://doi.org/10.1016/j.neuroimage.2019.116107.

Paret, C., Ruf, M., Gerchen, M.F., Kluetsch, R., Demirakca, T., Jungkunz, M., Ende, G., 2016. fMRI neurofeedback of amygdala response to aversive stimuli enhances prefrontal-limbic brain connectivity. Neuroimage 125, 182–188. https://doi.org/10.1016/j.neuroimage.2015.10.027.

Peters, H., Riedl, V., Manoliu, A., Scherr, M., Schwerthoffer, D., Zimmer, C., Koch, K., 2017. Changes in extra-striatal functional connectivity in patients with schizophrenia in a psychotic episode. Br. J. Psychiatry 210 (1), 75–82. https://doi.org/10.1192/bjp.bp.114.151928.

Pettersson-Yeo, W., Allen, P., Benetti, S., McGuire, P., Mechelli, A., 2011. Dysconnectivity in schizophrenia: where are we now? Neurosci. Biobehav. Rev. 35 (5), 1110–1124. https://doi.org/10.1016/j.neubiorev.2010.11.004.

Power, J.D., Barnes, K.A., Snyder, A.Z., Schlaggar, B.L., Petersen, S.E., 2012. Spurious but systematic correlations in functional connectivity MRI networks arise from subject motion. Neuroimage 59 (3), 2142–2154. https://doi.org/10.1016/j.neuroimage.2011.10.018.

Power, J.D., Lynch, C.J., Dubin, M.J., Silver, B.M., Martin, A., Jones, R.M., 2020. Characteristics of respiratory measures in young adults scanned at rest, including systematic changes and "missed" deep breaths. Neuroimage 204, 116234. https://doi.org/10.1016/j.neuroimage.2019.116234.

Power, J.D., Lynch, C.J., Gilmore, A.W., Gotts, S.J., Martin, A., 2019. Reply to Spreng et al.: multiecho fMRI denoising does not remove global motion-associated respiratory signals. Proc. Natl. Acad. Sci. U. S. A. https://doi.org/10.1073/pnas.1909852116.

Power, J.D., Plitt, M., Gotts, S.J., Kundu, P., Voon, V., Bandettini, P.A., Martin, A., 2018. Ridding fMRI data of motion-related influences: removal of signals with distinct spatial and physical bases in multiecho data. Proc. Natl. Acad. Sci. U. S. A. 115 (9), E2105–E2114. https://doi.org/10.1073/pnas.1720985115.

Power, J.D., Plitt, M., Laumann, T.O., Martin, A., 2017. Sources and implications of whole-brain fMRI signals in humans. Neuroimage 146, 609–625. https://doi.org/10.1016/j.neuroimage.2016.09.038.

Power, J.D., Schlaggar, B.L., Petersen, S.E., 2015. Recent progress and outstanding issues in motion correction in resting state fMRI. Neuroimage 105, 536–551. https://doi.org/10.1016/j.neuroimage.2014.10.044.

Qian, X., Castellanos, F.X., Uddin, L.Q., Loo, B.R.Y., Liu, S., Koh, H.L., Zhou, J., 2019. Large-scale brain functional network topology disruptions underlie symptom heterogeneity in children with attention-deficit/hyperactivity disorder. Neuroimage Clin 21, 101600. https://doi.org/10.1016/j.nicl.2018.11.010.

Raine, A., 1991. The SPQ: a scale for the assessment of schizotypal personality based on DSM-III-R criteria. Schizophr. Bull. 17 (4), 555–564. https://doi.org/10.1093/schbul/17.4.555.

Ramot, M., Kimmich, S., Gonzalez-Castillo, J., Roopchansingh, V., Popal, H., White, E., Martin, A., 2017. Direct modulation of aberrant brain network connectivity through real-time NeuroFeedback. Elife 6. https://doi.org/10.7554/eLife.28974.

Ruiz, S., Lee, S., Soekadar, S.R., Caria, A., Veit, R., Kircher, T., Sitaram, R., 2013. Acquired self-control of insula cortex modulates emotion recognition and brain network connectivity in schizophrenia. Hum. Brain Mapp. 34 (1), 200–212. https://doi.org/10.1002/hbm.21427.

Saad, Z.S., Gotts, S.J., Murphy, K., Chen, G., Jo, H.J., Martin, A., Cox, R.W., 2012. Trouble at rest: how correlation patterns and group differences become distorted after global signal regression. Brain Connect. 2 (1), 25–32. https://doi.org/10.1089/brain.2012.0080.

Schaefer, A., Kong, R., Gordon, E.M., Laumann, T.O., Zuo, X.N., Holmes, A.J., Yeo, B.T.T., 2018. Local-global parcellation of the human cerebral cortex from intrinsic functional connectivity MRI. Cerebr. Cortex 28 (9), 3095–3114. https://doi.org/10.1093/cercor/bhx179.

Shukla, D.K., Chiappelli, J.J., Sampath, H., Kochunov, P., Hare, S.M., Wisner, K., Hong, L.E., 2019. Aberrant frontostriatal connectivity in negative symptoms of schizophrenia. Schizophr. Bull. 45 (5), 1051–1059. https://doi.org/10.1093/schbul/sby165.

Spreng, R.N., Fernandez-Cabello, S., Turner, G.R., Stevens, W.D., 2019. Take a deep breath: multiecho fMRI denoising effectively removes head motion artifacts, obviating the need for global signal regression. Proc. Natl. Acad. Sci. U. S. A. https://doi.org/10.1073/pnas.1909848116.

Su, T.W., Lan, T.H., Hsu, T.W., Biswal, B.B., Tsai, P.J., Lin, W.C., Lin, C.P., 2013. Reduced neuro-integration from the dorsolateral prefrontal cortex to the whole brain and executive dysfunction in schizophrenia patients and their relatives. Schizophr. Res. 148 (1–3), 50–58. https://doi.org/10.1016/j.schres.2013.05.005.

Weiskopf, N., Veit, R., Erb, M., Mathiak, K., Grodd, W., Goebel, R., Birbaumer, N., 2003. Physiological self-regulation of regional brain activity using real-time functional magnetic resonance imaging (fMRI): methodology and exemplary data. Neuroimage 19 (3), 577–586.

Yamashita, A., Hayasaka, S., Kawato, M., Imamizu, H., 2017. Connectivity neurofeedback training can differentially change functional connectivity and cognitive performance. Cerebr. Cortex 27 (10), 4960–4970. https://doi.org/10.1093/cercor/bhx177.

Yang, G.J., Murray, J.D., Repovs, G., Cole, M.W., Savic, A., Glasser, M.F., Anticevic, A., 2014. Altered global brain signal in schizophrenia. Proc. Natl. Acad. Sci. U. S. A. 111 (20), 7438–7443. https://doi.org/10.1073/pnas.1405289111.

Yarkoni, T., Poldrack, R.A., Nichols, T.E., Van Essen, D.C., Wager, T.D., 2011. Large-scale automated synthesis of human functional neuroimaging data. Nat. Methods 8 (8), 665–670. https://doi.org/10.1038/nmeth.1635.

Yeo, B.T., Krienen, F.M., Sepulcre, J., Sabuncu, M.R., Lashkari, D., Hollinshead, M., Buckner, R.L., 2011. The organization of the human cerebral cortex estimated by intrinsic functional connectivity. J. Neurophysiol. 106 (3), 1125–1165. https://doi.org/10.1152/jn.00338.2011.

Young, K.D., Siegle, G.J., Misaki, M., Zotev, V., Phillips, R., Drevets, W.C., Bodurka, J., 2018. Altered task-based and resting-state amygdala functional connectivity following real-time fMRI amygdala neurofeedback training in major depressive disorder. Neuroimage Clin 17, 691–703. https://doi.org/10.1016/j.nicl.2017.12.004.

Zamoscik, V., Niemeyer, C., Gerchen, M.F., Fenske, S.C., Witthoft, M., Kirsch, P., 2017. [Sensory Inventory (SI): self-assessment of sensory sensitivity for adults and adolescents]. Fortschr. Neurol. Psychiatr. 85 (9), 541–551. https://doi.org/10.1055/s-0043-117885.

Zamoscik, V.E., Schmidt, S.N.L., Gerchen, M.F., Samsouris, C., Timm, C., Kuehner, C., Kirsch, P., 2018. Respiration pattern variability and related default mode network connectivity are altered in remitted depression. Psychol. Med. 48 (14), 2364–2374. https://doi.org/10.1017/S0033291717003890.

Zarahn, E., Aguirre, G.K., D'Esposito, M., 1997. Empirical analyses of BOLD fMRI statistics. I. Spatially unsmoothed data collected under null-hypothesis conditions. Neuroimage 5 (3), 179–197.

Zhao, Z., Yao, S., Li, K., Sindermann, C., Zhou, F., Zhao, W., Becker, B., 2019. Real-time functional connectivity-informed neurofeedback of amygdala-frontal pathways reduces anxiety. Psychother. Psychosom. 88 (1), 5–15. https://doi.org/10.1159/000496057.

Zilverstand, A., Sorger, B., Slaats-Willemse, D., Kan, C.C., Goebel, R., Buitelaar, J.K., 2017. fMRI neurofeedback training for increasing anterior cingulate cortex activation in adult attention deficit hyperactivity disorder. An exploratory randomized, single-blinded study. PloS One 12 (1), e0170795. https://doi.org/10.1371/journal.pone.0170795.

Zweerings, J., Hummel, B., Keller, M., Zvyagintsev, M., Schneider, F., Klasen, M., Mathiak, K., 2019. Neurofeedback of core language network nodes modulates connectivity with the default-mode network: a double-blind fMRI neurofeedback study on auditory verbal hallucinations. Neuroimage 189, 533–542. https://doi.org/10.1016/j.neuroimage.2019.01.058.